Output Stream of Leaky Integrate-and-Fire Neuron Without Diffusion Approximation

Alexander K. Vidybida

Journal of Statistical Physics
1

ISSN 0022-4715

J Stat Phys
DOI 10.1007/s10955-016-1698-2

Volume 165 • Number 6 • Decem

ONLINE FIRST

Journal of Statistical Physics

10955 • ISSN 0022-4715
165(6) 991–1180 (2016)

Springer

Springer

J Stat Phys
DOI 10.1007/s10955-016-1698-2

Output Stream of Leaky Integrate-and-Fire Neuron Without Diffusion Approximation

Alexander K. Vidybida[1]

Received: 12 May 2016 / Accepted: 9 December 2016

Abstract Probability density function (pdf) of output interspike intervals (ISI) as well as mean ISI is found in exact form for leaky integrate-and-fire (LIF) neuron stimulated with Poisson stream. The diffusion approximation is not used. The whole range of possible ISI values is represented as infinite union of disjoint intervals: $]0;\infty[=]0;T_2]+\sum_{m=0}^{\infty}]T_2+m\,T_3;T_2+(m+1)T_3]$, where T_2 and T_3 are defined by the LIF's physical parameters. Exact expression for the obtained pdf is different on different intervals and is given as finite sum of multiple integrals. For the first three intervals the integrals are taken which brings about exact expressions with polylogarithm functions. The found distribution can be bimodal for some values of parameters. Conditions, which ensure bimodality are briefly analyzed.

Keywords LIF neuron · Poisson stochastic process · Probability density function · Output intensity

Mathematics Subject Classification 60G55 · 60G10 · 60K15 · 60K40 · 92B20

1 Introduction

The leaky integrate-and-fire (LIF) neuron [2], is a widely used model in theoretical neuroscience, which is due to its simplicity, see Sect. 2.1. At the same time, the problem of finding the probability density function (pdf) of the output stream of interspike intervals (ISIs) of LIF neuron under Poisson stimulation is not solved exactly. Partially, this may be explained by the fact that any input impulse decays exponentially and its remnant is present in the neuron until next firing. Numerous results regarding description of the output stream are obtained

---

A short version of this paper was published in Ukrainian [1].

✉ Alexander K. Vidybida
vidybida@bitp.kiev.ua
http://vidybida.kiev.ua

[1] Bogolyubov Institute for Theoretical Physics, Metrologichna str., 14-B, Kiev 03680, Ukraine

in diffusion approximation, see review [3]. In the diffusion approximation, the time course of the membrane potential (the degree of excitation) is described as the Ornstein–Uhlenbeck stochastic process [4]. In this approach, the mean output ISI and dispersion can be calculated. As regards the ISI pdf, the only found expressions are approximate, due to difficulties in calculation of the first passage times distribution for the Ornstein–Uhlenbeck stochastic process, see [5].

The usage of diffusion approximation is approved if a large number of input impulses, delivered in a short period of time, is necessary to trigger a neuron. This situation is realistic for some biological neurons [6]. For some biological neurons triggering can be achieved with a small number of input impulses, starting from two, see [7,8]. For those neurons description in terms of diffusion approximation cannot be approved.

In the interesting paper [9], ISI pdf is calculated without diffusion approximation as well. In that paper, instead of expecting that excitation decays in time exponentially (see Eq. 5) it is assumed that input impulse is stored unchanged in the neuron during random time interval after which it disappears. At first glance, this is serious deviation from the deterministic exponential decay (Eq. 5), pertinent for real neurons. But for triggering the time course of compound postsynaptic potential is essential. Under the assumptions of [9] the time course is approximated with a step-like function. This approximation is the more precise the more impulses are required for triggering. In [9], the found pdf matches experimental one if output ISI is longer than 60 ms. During this time a large number of input impulses can arrive to neuron. This explains good fit with experimental histograms obtained in [9].

In this paper, the ISI's pdf and mean output ISI are calculated in exact form without usage of diffusion approximation. Calculations are made for the least favorable for diffusion approximation case when already two input impulses are able to trigger neuron, provided that the impulses are applied with a short time interval, see condition (1). Exact value of the pdf for a concrete ISI length t is obtained as a finite sum of multiple integrals.

2 Statement of the Problem

2.1 Definition of Leaky Integrate-and-Fire Neuron

The LIF neuronal model used in this paper is a simplest one. It is characterized with three positive constants:

1. τ is the relaxation time,
2. V_0 is the firing threshold,
3. h is the input impulse height.

As regards h and V_0, we hypothesize the following condition:

$$0 < h < V_0 < 2h. \tag{1}$$

At any moment $l \in [0; \infty[$, the LIF's state is described with a non-negative number $V(l)$, which is interpreted as deviation of trans-membrane potential from the resting state in the direction of depolarization, or in other words, the degree of excitation. Here we expect that $V = 0$ at the resting state, and $V > 0$ in the presence of depolarization/excitation.

Stimulation is due to input impulses. An input impulse received at moment l advances $V(l)$ by h:

$$V(l) \to V(l) + h. \tag{2}$$

Here we expect that input impulses are delivered to the LIF neuron from a Poisson stream of intensity λ. Among several equivalent descriptions of Poisson stochastic process (see e.g. [10, Chap. II, § 9]) we chose the following one. Possible trajectories of Poisson process are given through consecutive moments $\{l_1, l_2, \dots, l_k, \dots\}$ of receiving input impulses,

$$0 < l_1 < l_2 < \cdots < l_k < \cdots . \tag{3}$$

Poissonian measure on cylinder sets of trajectories is defined as usual:

$$e^{-\lambda l_1}\lambda dl_1 e^{-\lambda(l_2-l_1)}\lambda dl_2 \dots e^{-\lambda(l_k-l_{k-1})}\lambda dl_k. \tag{4}$$

The leakage in the LIF means that without stimulation $V(l)$ decays exponentially:

$$V(l+s) = V(l)e^{-\frac{s}{\tau}}, \qquad s > 0. \tag{5}$$

LIF is characterized with the threshold value of excitation, V_0. The latter means that once the following condition is fulfilled: $V(l) > V_0$, the LIF fires a spike (sends output impulse) and appears in its resting state, $V(l) = 0$.

It follows from (5) and (2) that LIF may fire only at moments of receiving input impulses. Condition (1) means that a single input impulse applied to LIF in its resting state cannot trigger firing, but already two input impulses applied in a short succession are able to trigger.

Calculation methods used here are transparent enough if limitation (1) is imposed. This does not exclude applicability of our methods when, instead of (1), another condition, like $2h \le V_0 < 3h$ or so, is fulfilled. At the same time, without condition (1) fulfilled one could expect additional combinatorial difficulties in calculations. On the other hand, used here condition (1) is the least favorable for usage of diffusion approximation.

2.2 Output Stream

When a LIF neuron is subjected to Poisson stimulation, it sends output impulses in some moments. Our task is to characterize the output stream.

Notice that neuron appears in its standard state with $V = 0$ after each firing. The state of the input stream (Poisson stream) is the same all the time. Therefore, the output stream must be a renewal process. For our use it is enough to know its ISI's pdf $P(t)$. Expression $P(t)\,dt$ gives probability to have an ISI duration within $[t; t+dt[$. This probability can be found as probability that the first triggering happens t units of time after switching on, provided that at the switching on moment (starting of the epoch), LIF is at its resting state: $V(0) = 0$.

The problem of calculating $P(t)$ in our case belongs to a class of boundary tasks for stochastic processes, and can be reduced to the first passage problem for crossing the level V_0. This type of tasks are pertinent for mass service theory, risk assessment and others. One model used in this area is the compound Poisson process with drift (CPPD). In particular, CPPD model is used in [11, p. 125] for description of neuronal activity (see also Sect. 6). The approach of [11] is not suitable in situation denoted in (5) (the presence of electric loss).

3 Existence and Continuity of $P(t)$

The first impulse after switching on is generated at moment t if and only if the following two independent events take place. The first event is that all input impulses received between 0 and t do not trigger the neuron, but create such an excitation ($V(t)$) at time t, that an impulse received at the moment t triggers the neuron. Actually, that means that $V(t) > V_0 - h$. The second event is receiving impulse during $[t; t + dt[$. If $\widetilde{P}(t)$ denotes the probability of the first event, then

$$P(t)dt = \widetilde{P}(t)\lambda dt.$$

Definition 1 A sequence of k input impulses, or moments of their arrival $\{l_1, l_2, \dots, l_k\}$, is called a silent k-sequence if our LIF neuron does not fire starting from its resting state during receiving the whole sequence of that k input impulses.

Let $\mathbb{M}_{k,t}$, where $k = 1, 2, \dots$ and $t > 0$, denote an event that the first k input impulses, $\{l_1, l_2, \dots, l_k < t\}$, compose a silent k-sequence and create such excitation in the LIF, that arrival of the next one at moment $l_{k+1} \in [t; t + dt[$ triggers it. The letter means that $V(t) > V_0 - h$. Let $\widetilde{P}_k(t)$ denote the probability of $\mathbb{M}_{k,t}$.

Theorem 1 *The probability $\widetilde{P}_k(t)$ exists and it is a continuous function of t.*

Proof Let $\mathscr{V}_{l_1 \dots l_i}(x)$ denote the following function:

$$\mathscr{V}_{l_1 \dots l_i}(x) = h \sum_{j=1}^{i} e^{-(x - l_j)/\tau}. \tag{6}$$

If $\{l_1 \dots l_i\}$ is a silent sequence and $x > l_i$, then $\mathscr{V}_{l_1 \dots l_i}(x)$ gives the level of excitation at moment x if input impulses are obtained at moments $\{l_1, \dots, l_i\}$.

The left hand part in Eq. (6) suggests that $\mathscr{V}_{l_1 \dots l_i}(x)$ is a function from $\mathbb{R}^1$ to $\mathbb{R}^1$ with parameters $(l_1, \dots, l_i) \in \mathbb{R}^i$. At the same time nothing prevents us from interpreting $\mathscr{V}_{l_1 \dots l_i}(x)$ as a function from $\mathbb{R}^{i+1}$ to $\mathbb{R}^1$ with an argument $(l_1, \dots, l_i, x)$. Further, $\mathscr{V}_{l_1 \dots l_i}(x)$ can be as well interpreted as a function from infinite-dimensional space $\mathbb{R}^{\mathbb{N}}$ to $\mathbb{R}^1$, which takes into account only the first $i + 1$ coordinates of a point in the $\mathbb{R}^{\mathbb{N}}$. The latter interpretation is used after Eq. (9).

A sequence $\{l_1, l_2, \dots, l_k\}$ is silent if and only if the following conditions are satisfied:

$$\mathscr{V}_{l_1}(l_2) \le V_0 - h, \quad \mathscr{V}_{l_1 l_2}(l_3) \le V_0 - h, \ \dots, \ \mathscr{V}_{l_1 \dots l_{k-1}}(l_k) \le V_0 - h. \tag{7}$$

Further, an impulse at moment $l_{k+1} \in [t; t + dt[$ will trigger if and only if in addition to (7) the following conditions are satisfied:

$$l_k < t, \tag{8}$$

$$\mathscr{V}_{l_1 \dots l_k}(t) > V_0 - h. \tag{9}$$

The set $M_{k,t}$ of realizations of Poisson process, which corresponds to event $\mathbb{M}_{k,t}$, is defined in $\mathbb{R}^{\mathbb{N}}$ by conditions (3), (7), (8) and (9). Since all those conditions are formulated by means of inequalities composed of continuous from $\mathbb{R}^{\mathbb{N}}$ to $\mathbb{R}^1$ functions, then $M_{k,t}$ is a Borel set and $\mathbb{M}_{k,t}$ is a correct (measurable) event. Thus, $\widetilde{P}_k(t)$ exists.

In order to prove continuity of $\widetilde{P}_k(t)$ one has to estimate the difference

$$|\widetilde{P}_k(t + \Delta t) - \widetilde{P}_k(t)|. \tag{10}$$

This difference is equal to the difference of measures (4) of sets $M_{k,t}$ and $M_{k,t+\Delta t}$. The latter difference does not exceed the measure of any of two sets: $M_{k,t+\Delta t} \backslash M_{k,t}$ and $M_{k,t} \backslash M_{k,t+\Delta t}$.

The set $M_{k,t+\Delta t} \backslash M_{k,t}$ is defined by (3), (7) and the following conditions:

$$t \le l_k < t + \Delta t, \quad \mathscr{V}_{l_1 \dots l_k}(t + \Delta t) > V_0 - h.$$

First of these conditions ensures that measure (4) of $M_{k,t+\Delta t}\backslash M_{k,t}$ is of order $O(\Delta t)$.

The set $M_{k,t}\backslash M_{k,t+\Delta t}$ is defined by (3), (7) and the following conditions:

$$\mathscr{V}_{l_1\ldots l_k}(t) > V_0 - h, \quad \mathscr{V}_{l_1\ldots l_k}(t+\Delta t) \le V_0 - h.$$

Taking into account (6), the latter can be presented as follows:

$$V_0 - h < \mathscr{V}_{l_1\ldots l_k}(t) \le e^{\Delta t/\tau}(V_0 - h). \tag{11}$$

Let $M_{\Delta t}$ denote a set in $\mathbb{R}^{\mathbb{N}}$, composed of all such points $\{l_1, \ldots, l_k, \ldots\}$ from $\mathbb{R}^{\mathbb{N}}$ that their first k coordinates $\{l_1, \ldots, l_k\}$ satisfy (11). $M_{\Delta t}$ is a correct event and $M_{\Delta t} \supset M_{k,t}\backslash M_{k,t+\Delta t}$. Thus, measure (4) of $M_{k,t}\backslash M_{k,t+\Delta t}$ does not exceed measure of $M_{\Delta t}$. Additionally $\Delta t_2 > \Delta t_1 \Rightarrow M_{\Delta t_2} \supset M_{\Delta t_1}$ and $\bigcap\limits_{\Delta t>0} M_{\Delta t} = \emptyset$. It follows from the latter that measure of $M_{\Delta t}$ converges to zero if $\Delta t \to 0$, and the same takes place for $M_{k,t}\backslash M_{k,t+\Delta t}$. Thus, the difference (10) converges to zero if $\Delta t \to 0$, and continuity of $\widetilde{P}_k(t)$ is proven. □

Theorem 2 *ISI's probability density function $P(t)$ exists and it is continuous in t.*

Proof It is evident that the input impulse, which causes the first triggering, may have number $n = 2, 3, \ldots$, and events with different n are disjoint. Therefore

$$P(t)dt = \sum_{k\ge1} \widetilde{P}_k(t)\lambda dt. \tag{12}$$

With t fixed, the sum (12) is finite. Indeed, if two isolated impulses do not trigger, then those impulses are separated in time by not less than T_2 units of time, where T_2 is defined by the following condition $he^{-T_2/\tau} = V_0 - h$, or

$$T_2 = \tau \ln \frac{h}{V_0 - h}. \tag{13}$$

If additional impulses are received before those two, then those two must be separated by an interval even longer than T_2. Thus, for any t there is such a k_{max}, that it is impossible to allocate within $]0; t[$ a silent m-sequence with $m > k_{max}$, and $\widetilde{P}_m(t') = 0$ for $t' \in]0; t[$. Therefore, $P(t)$ is correctly defined by (12). □

In order to prove the continuity, we have to figure out exactly which terms are present in (12) for any t. For this purpose let us define interval T_3 by the following condition: $V_0e^{-T_3/\tau} = V_0 - h$, or

$$T_3 = \tau \ln \frac{V_0}{V_0 - h}. \tag{14}$$

The set of all possible ISI values can be now represented as union of disjoint subsets:

$$]0; \infty[=]0; T_2] + \sum_{m=3}^{\infty}]\Theta_m; \Theta_{m+1}], \tag{15}$$

where

$$\Theta_m = T_2 + (m-3)T_3, \quad m = 3, 4, \ldots, \quad \Theta_2 = 0.$$

If we define as $l_k - l_1$ the length of sequence $\{l_1, l_2, \ldots, l_k\}$, then Θ_m is the minimal possible length of silent $(m-1)$-sequence. Indeed, the sequence with

$$l_1 = 0, \quad l_2 = \Theta_3, \; \ldots, \; l_{m-1} = \Theta_m \tag{16}$$

is silent. Indeed, from the definitions of T_2, T_3 it follows that for the sequence (16) the following equations hold:

$$\mathscr{V}_{l_1}(l_2) = V_0 - h, \quad \mathscr{V}_{l_1 l_2}(l_3) = V_0 - h, \ \ldots, \ \mathscr{V}_{l_1 \ldots l_{m-2}}(l_{m-1}) = V_0 - h. \tag{17}$$

Decreasing of temporal distance between any two consecutive impulses will result in replacing "$= V_0 - h$" with "$> V_0 - h$" somewhere in (17), and in triggering with arrival of second impulse from those two. Therefore, one can rewrite (12) as follows

$$P(t)dt = \sum_{k=1}^{m-1} \widetilde{P}_k(t)\lambda dt, \quad t \in]\Theta_m; \Theta_{m+1}], \quad m = 2, 3, \ldots. \tag{18}$$

From (18) it follows that $P(t)$ is continuous at intervals $]\Theta_m; \Theta_{m+1}[$ as finite sum of continuous functions. To complete, it is necessary to prove continuity in the points Θ_{m+1}, $m = 2, 3, \ldots$. For this purpose it is enough to prove the following

$$\widetilde{P}_m(\Theta_{m+1}) = 0, \quad m = 2, 3, \ldots. \tag{19}$$

The latter follows from the fact that Θ_{m+1} is the shortest length of a silent m-sequence. A silent m-sequence, which can be allocated on $[0; \Theta_{m+1}]$ is unique. Its arrival moments are defined in (16), and $l_m = \Theta_{m+1}$. Therefore, the cylinder set $M_{m,\Theta_{m+1}}$ has a single point from $\mathbb{R}^m$ as the cylinder base, and probability of the event $\mathbb{M}_{m,\Theta_{m+1}}$ equals zero, which proves (19). ☐

4 Form of Terms in (18)

For $k = 2, 3, \ldots$ let us introduce the following notations

$P_k^0(t)\lambda dt$	is the probability to receive a k-sequence $\{l_1, \ldots, l_{k-1}, l_k \in [t; t+dt[\}$ such that $\{l_1, \ldots, l_{k-1}\}$ is silent.
$P_k^-(t)\lambda dt$	is the probability to receive silent k-sequence $\{l_1, \ldots, l_{k-1}, l_k \in [t; t+dt[\}$.

It is clear that

$$P_k^0(t) = 0 \quad \text{if} \quad t \in]0; \Theta_k], \qquad P_k^-(t) = 0 \quad \text{if} \quad t \in]0; \Theta_{k+1}],$$

and

$$\widetilde{P}_k(t)\lambda dt = P_{k+1}^0(t)\lambda dt - P_{k+1}^-(t)\lambda dt.$$

By utilizing the latter, one can rewrite (18) as follows:

$$P(t)dt = \sum_{k=2}^{m-1} \left(P_k^0(t)\lambda dt - P_k^-(t)\lambda dt\right) + P_m^0(t)\lambda dt, \ t \in]\Theta_m; \Theta_{m+1}], \ m \geq 2. \tag{20}$$

In particular, $P(t)dt = P_2^0(t)\lambda dt$ if $t \in]\Theta_2; \Theta_3]$, where

$$P_2^0(t)\lambda dt = \lambda t e^{-\lambda t}\lambda dt. \tag{21}$$

Notice that if for $s > \Theta_{k+1}$ the expression $P_k^-(s)\lambda ds$ gives probability to receive silent k-sequence $\{l_1, \ldots, l_{k-1}, l_k \in [s; s+ds[\}$, then the expression $P_k^-(s)\lambda ds\, e^{-\lambda(t-s)}\lambda\, dt$ for $t > s$ gives probability to receive a $(k+1)$-sequence $\{l_1, \ldots, l_{k-1}, l_k \in [s; s+ds[, l_{k+1} \in$

$[t; t+dt[\}$ such that the subsequence of its first k arrival times is silent. Therefore, the following relation holds:

$$\int_{\Theta_{k+1}}^{t} P_k^-(s)\lambda\, ds\, e^{-\lambda(t-s)}\lambda\, dt = P_{k+1}^0(t)\lambda\, dt, \quad t \geq \Theta_{k+1}, \quad k = 2, 3, \dots . \tag{22}$$

Thus, calculation of terms in the sum (20) is reduced to calculation of exact expressions for $P_k^-(t)$, $k = 2, 3, \dots$. Below, we derive exact expressions for these functions through multiple integrals. Calculation of the integrals themselves is performed in the next section for $k = 2, 3$.

It was already noted that $P_k^-(t) = 0$ if $t \in]0; \Theta_{k+1}]$, and for $t = \Theta_{k+1}$ there is exactly one silent k-sequence $\{l_1, \dots, l_{k-1}, l_k = t\}$, namely, $\{\Theta_2, \Theta_3, \dots, \Theta_{k+1}\}$. For $t > \Theta_{k+1}$ the probability to get a silent k-sequence of type $\{l_1, \dots, l_{k-1}, l_k \in [t; t+dt[\}$ is strictly positive. In order to calculate that probability one has to integrate the expression

$$e^{-\lambda l_1}\lambda dl_1 e^{-\lambda(l_2-l_1)}\lambda dl_2 \dots e^{-\lambda(t-l_{k-1})}\lambda dt$$

over the set of coordinates $l_1, l_2, \dots, l_{k-1}$ such that there is no triggering at moments of time $l_1, l_2, \dots, l_{k-1}, t$:

$$P_k^-(t)\lambda dt = e^{-\lambda t}\lambda^k dt \int_{\underline{l_1}}^{\overline{l_1}} dl_1 \int_{\underline{l_2}}^{\overline{l_2}} dl_2 \dots \int_{\underline{l_{k-1}}}^{\overline{l_{k-1}}} dl_{k-1}, \tag{23}$$

where upper and lower limits in integrals still have to be defined.

The lower limits can be determined from condition that input impulses at moments $l_1, l_2, \dots, l_{k-1}, t$ should not trigger the neuron. It is clear, that $\underline{l_1} = 0$. In general case, $\underline{l_{i+1}}(l_1, \dots, l_i)$ can be determined from the following condition: $\mathcal{V}_{l_1 \dots l_i}(\underline{l_{i+1}}) = V_0 - h$, which gives

$$\underline{l_{i+1}}(l_1, \dots, l_i) = T_2 + \tau \ln\left(\sum_{j=1}^{i} e^{l_j/\tau}\right), \quad i = 1, \dots, k-2. \tag{24}$$

The upper limits in (23) depend additionally on k and t: $\overline{l_{i+1}} = \overline{l_{i+1}}(k, t, l_1, \dots, l_i)$. The value of $\overline{l_{i+1}}(k, t, l_1, \dots, l_i)$ must be chosen in such a way that ensures a possibility to allocate moments $l_{i+2}, \dots, l_{k-1}, t$ in such a way that resulting k-sequence $\{l_1, \dots, l_i, \overline{l_{i+1}}, l_{i+2}, \dots, l_{k-1}, t\}$ will be silent.

To figure out $\overline{l_{i+1}}(k, t, l_1, \dots, l_i)$ with already fixed $l_1, \dots, l_i$ and t it is worth noticing that non-trigger condition implies that if the biggest possible values for $\overline{l_{i+1}}, l_{i+2}, \dots, l_{k-1}$ are chosen, then:

$$\begin{aligned} \mathcal{V}_{l_1 \dots l_i\, \overline{l_{i+1}}}(l_{i+2}) &= V_0 - h, \\ &\dots \\ \mathcal{V}_{l_1 \dots l_i\, \overline{l_{i+1}}\, l_{i+2} \dots l_{k-1}}(t) &= V_0 - h. \end{aligned} \tag{25}$$

From the latter it follows that for the biggest possible values of $\overline{l_{i+1}}, l_{i+2}, \dots, l_{k-1}$ the following equations are valid, see Fig. 1:

$$l_{i+3} - l_{i+2} = l_{i+4} - l_{i+3} = \dots = t - l_{k-1} = T_3.$$

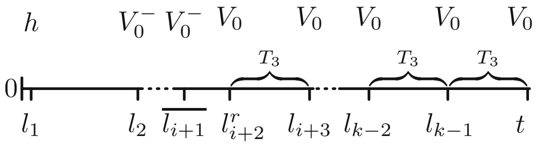

Fig. 1 Disposition of time moments for determining $\overline{l_{i+1}}(k, t, l_1, \dots, l_i)$. The *upper row* indicates the value of depolarization at each moment after receiving input impulse at that moment. Here $V_0^- \le V_0$ and $T_2 < l^r_{i+2} - \overline{l_{i+1}}$

Thus, the biggest possible value for l_{i+2} is as follows:

$$l^r_{i+2} = t - (k - i - 2)T_3.$$

$\overline{l_{i+1}}(k, t, l_1, \dots, l_i)$ can be now found if we substitute l^r_{i+2} for l_{i+2} in the (25):

$$\overline{l_{i+1}}(k, t, l_1, \dots, l_i) = \tau \ln \left(e^{(t-\Theta_{k+1-i})/\tau} - \sum_{j=1}^{i} e^{l_j/\tau} \right), \quad i = 0, \dots, k-2. \tag{26}$$

Equations (23), (24), (26) give the exact expressions for probabilities $P_k^-(t)\lambda dt$, $k = 2, \dots$.

4.1 Calculation of the First Terms in (20)

We calculate[1] here exact expressions for the $P(t)dt$ at first domains of the partition (15). Calculations in accordance with Eq. (23) with $k = 2$, or $k = 3$ give the following:

$$P_2^-(t) = e^{-\lambda t}\lambda(t - T_2), \quad t \ge \Theta_3, \tag{27}$$

$$\begin{aligned} P_3^-(t) = {} & e^{-\lambda t}\lambda^2 \left((t - 2T_2)(t - \Theta_4) - \frac{1}{2}(t - \Theta_4)^2 \right) \\ & + e^{-\lambda t}(\tau\lambda)^2 \left(\mathrm{Li}_2\left(e^{(T_2-t)/\tau}\right) - \mathrm{Li}_2\left(e^{-T_3/\tau}\right) \right), \quad t \ge \Theta_4, \end{aligned} \tag{28}$$

where Li_2 denote dilogarithm.

The resting terms in (20) for $t \le \Theta_5$ can be found with the help of Eqs. (27), (28) and (22):

$$P_3^0(t) = e^{-\lambda t}\frac{\lambda^2(t - T_2)^2}{2}, \quad t \ge \Theta_3, \tag{29}$$

$$\begin{aligned} P_4^0(t) = {} & e^{-\lambda t}\frac{\lambda^3}{6}(\Theta_4 - t)^2(2T_3 - 4T_2 + t) \\ & + e^{-\lambda t}\tau^2\lambda^3(\Theta_4 - t)\mathrm{Li}_2\left(e^{-T_3/\tau}\right) \\ & + e^{-\lambda t}(\tau\lambda)^3 \left(\mathrm{Li}_3\left(e^{-T_3/\tau}\right) - \mathrm{Li}_3\left(e^{(T_2-t)/\tau}\right) \right), \quad t \ge \Theta_4, \end{aligned} \tag{30}$$

where Li_3 denote trilogarithm.

---

[1] Calculations are made with the help of free computer algebra system maxima (`maxima.sourceforge.net`).

Exact expressions (21), (27)–(30) give exact expressions for (20) at the initial part of t values:

$$P(t)dt = \begin{cases} P_2^0(t)\lambda dt, & t \in]0; T_2], \\ \left(P_2^0(t) - P_2^-(t) + P_3^0(t)\right)\lambda dt, & t \in]T_2; T_2 + T_3], \\ \left(\sum\limits_{k=2}^{3}\left(P_k^0(t) - P_k^-(t)\right) + P_4^0(t)\right)\lambda dt, & t \in]T_2 + T_3; T_2 + 2T_3], \end{cases} \tag{31}$$

where T_2, T_3 are given by Eqs. (13), (14). A graph of the expressions (31) is shown in Fig. 2a.

Also, for the checking purpose, the $P(t)$ for $t \in]0; \Theta_5]$ was calculated numerically, by means of Monte Carlo method. In the Monte Carlo calculations, we use the Mersenne Twister random number generator implemented in the GNU Scientific Library (https://www.gnu.org/software/gsl/-). The result is shown in Fig. 2b. See also examples in Fig. 3.

5 Mean Interspike Interval

The mean ISI $\bar{t}$ can be calculated as follows:

$$\bar{t} \equiv \int\limits_0^\infty t P(t)dt,$$

or, taking into account Eq. (20):

$$\bar{t} = \sum_{m=2}^{\infty} \int\limits_{\Theta_m}^{\Theta_{m+1}} t \left(\sum_{k=2}^{m-1}\left(P_k^0(t) - P_k^-(t)\right) + P_m^0(t)\right)\lambda dt. \tag{32}$$

It can be proven that in (32) the terms with sign "plus" compose an absolutely convergent series, and the same is valid for terms with sign "minus". This allows arbitrary regrouping of terms in (32) without changing the whole series value. In particular, after a suitable regrouping one has:

$$\bar{t} = \int\limits_0^\infty t\ P_2^0(t)\lambda dt + \sum_{m=3}^{\infty}\int\limits_{\Theta_m}^{\infty} t\ \left(P_m^0(t) - P_{m-1}^-(t)\right)\lambda dt. \tag{33}$$

Taking into account (21) and (22) in (33) gives after integration by parts:

$$\bar{t} = \frac{2}{\lambda} + \frac{1}{\lambda}\sum_{m=3}^{\infty}\int\limits_{\Theta_m}^{\infty} P_{m-1}^-(t)\lambda dt. \tag{34}$$

From the definition of $P_{m-1}^-(t)$ it follows that $\int_{\Theta_m}^\infty P_{m-1}^-(t)\lambda dt$ is the probability that the first $m-1$ input impulses compose a silent $(m-1)$-sequence. Thus

$$\int_{\Theta_m}^{\infty} P_{m-1}^-(t)\lambda dt = \lambda^{m-1}\int\limits_0^\infty dl_1 \int\limits_{\underline{l_2}}^\infty dl_2 \ldots \int\limits_{\underline{l_{m-1}}}^\infty dl_{m-1} e^{-\lambda l_{m-1}}. \tag{35}$$

Equation (35) can also be proven formally by substituting there $P_{m-1}^-(t)$ as given in (23) and reversing the integration order with respect to t and l_i, $i = 1, \ldots, m-2$, $m-2$ times. With

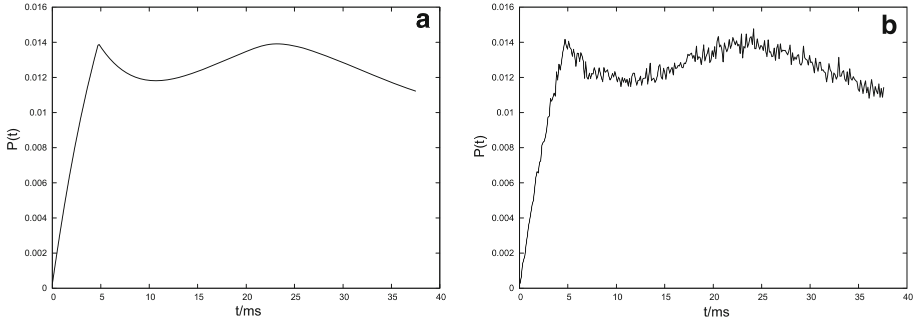

Fig. 2 Pdf of ISIs, $P(t)$, **a** found analytically by means of (31); **b** found numerically, by Monte Carlo simulation (used 1,000,000 output ISIs). Here $\lambda = 62.5\ \mathrm{s}^{-1}$, $\tau = 20$ ms, $V_0 = 20$ mV, $h = 11.2$ mV. The total probability mass under the curve drawn ($0 \le t \le \Theta_5 = 37.66$ ms) is 0.454. The coefficient of determination between the two curves is $R^2 = 0.981105$

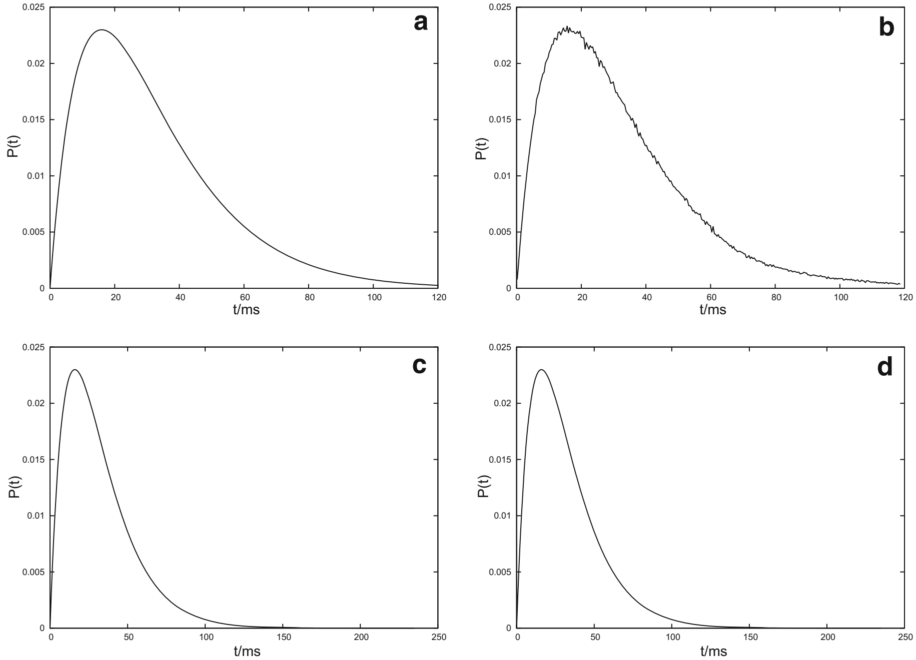

Fig. 3 Examples of pdf for different parameter values found analytically (**a**, **c**) and numerically, by Monte Carlo simulation (**b**, **d**). In **a**, **b** $\tau = 20$ ms, the curve's domain is $[0; \Theta_4]$, the total probability mass under the curve drawn is 0.990811, $R^2 = 0.998983$. In **c**, **d** $\tau = 80$ ms, the curve's domain is $[0; \Theta_3]$, the total probability mass under the curve drawn is 0.999994, $R^2 = 0.998991$. In **a**–**d** $\lambda = 62.5\ \mathrm{s}^{-1}$, $V_0 = 20$ mV, $h = 19$ mV, the number of output spikes used in Monte Carlo simulations is 1,000,000. Notice, that in the simulations, only those generated ISIs contribute to calculation of corresponding curve, which fall into its domain. This explains why curve in Fig. 2b is considerably less regular than those displayed here (**b**, **d**), in spite of the same number of output spikes generated

the following notation

$$\mathscr{P}_k = \lambda^k \int\limits_0^{\infty} dl_1 \int\limits_{\underline{l_2}}^{\infty} dl_2 \dots \int\limits_{\underline{l_k}}^{\infty} dl_k e^{-\lambda l_k}, \tag{36}$$

Eq. (34) takes the following form:

$$\bar{t} = \frac{2}{\lambda} + \frac{1}{\lambda} \sum_{m=3}^{\infty} \mathscr{P}_{m-1}. \tag{37}$$

In order to calculate integrals $\mathscr{P}_k$ it is necessary to use explicit expressions (24) for functions $\underline{l_{i+1}}(l_1, \dots, l_i)$, or the following equivalent expressions:

$$\sum_{j=1}^{i} e^{l_j/\tau} = a\, e^{\underline{l_{i+1}}/\tau}, \quad i = 1, 2, \dots, k-1, \tag{38}$$

where

$$a = \frac{V_0 - h}{h}, \quad 0 < a < 1.$$

Use in (36) the following substitution of variables:

$$x_i = e^{\frac{l_i}{\tau}}, \qquad dl_i = \tau \frac{dx_i}{x_i}, \qquad i = 1, 2, \dots, k. \tag{39}$$

Then the lower limits of integration and the integrand turn into the following:

$$\underline{l_i} = \frac{1}{a} \sum_{j=1}^{i-1} x_j, \quad i = 2, 3, \dots, k, \qquad e^{-\lambda l_k} = \frac{1}{(x_k)^{\lambda\tau}},$$

and

$$\mathscr{P}_k = (\lambda\tau)^k \int\limits_1^{\infty} \frac{dx_1}{x_1} \int\limits_{\frac{1}{a}x_1}^{\infty} \frac{dx_2}{x_2} \dots \int\limits_{\frac{1}{a}\sum\limits_{j=1}^{k-1} x_j}^{\infty} \frac{dx_k}{{x_k}^{\lambda\tau+1}}, \quad k = 2, 3, \dots. \tag{40}$$

In particular,

$$\mathscr{P}_2 = (\lambda\tau)^2 \int\limits_1^{\infty} \frac{dx_1}{x_1} \int\limits_{\frac{1}{a}x_1}^{\infty} \frac{dx_2}{x_2^{\lambda\tau+1}} = a^{\lambda\tau}. \tag{41}$$

Now, the task of calculating the mean ISI is reduced to finding all terms $\mathscr{P}_k$ in accordance with Eq. (40). Let us calculate in (40) the rightmost integral:

$$\mathscr{P}_k = (\lambda\tau)^{k-1} \int\limits_1^{\infty} \frac{dx_1}{x_1} \int\limits_{\frac{1}{a}x_1}^{\infty} \frac{dx_2}{x_2} \dots \int\limits_{\frac{1}{a}\sum\limits_{j=1}^{k-2} x_j}^{\infty} \frac{dx_{k-1}}{x_{k-1}} \frac{a^{\lambda\tau}}{\left(\sum_{j=1}^{k-1} x_j\right)^{\lambda\tau}}, \quad k = 3, 4, \dots. \tag{42}$$

Now, replace $k-1$ with k' in (42) and omit prime in k':

$$\mathscr{P}_{k+1} = (\lambda\tau)^k a^{\lambda\tau} \int\limits_1^\infty \frac{dx_1}{x_1} \int\limits_{\frac{1}{a}x_1}^\infty \frac{dx_2}{x_2} \dots \int\limits_{\frac{1}{a}\sum\limits_{j=1}^{k-1} x_j}^\infty \frac{dx_k}{x_k\left(x_k + \sum\limits_{j=1}^{k-1} x_j\right)^{\lambda\tau}}, \quad k = 2, 3, \dots. \tag{43}$$

Let us denote

$$s_k = \sum_{j=1}^{k} x_j, \quad \lambda\tau = r.$$

Then, instead of (43) one has

$$\mathscr{P}_{k+1} = r^k a^r \int\limits_1^\infty \frac{dx_1}{x_1} \int\limits_{\frac{1}{a}x_1}^\infty \frac{dx_2}{x_2} \dots \int\limits_{\frac{1}{a}s_{k-1}}^\infty \frac{dx_k}{x_k\left(x_k + s_{k-1}\right)^{r}}, \quad k = 2, 3, \dots.$$

In the rightmost integral, perform substitution of variable as follows:

$$z = \left(\frac{x_k}{s_{k-1}} + 1\right)^{-1}.$$

The result is as follows:

$$\mathscr{P}_{k+1} = r^k a^r \int\limits_1^\infty \frac{dx_1}{x_1} \int\limits_{\frac{1}{a}x_1}^\infty \frac{dx_2}{x_2} \dots \int\limits_{\frac{1}{a}s_{k-2}}^\infty \frac{dx_{k-1}}{x_{k-1}\left(x_{k-1} + s_{k-2}\right)^{r}} I(a,r), \quad k = 3, 4 \dots, \tag{44}$$

where

$$I(a,r) = \int\limits_0^{\frac{a}{a+1}} \frac{z^{r-1}}{1-z}\, dz. \tag{45}$$

Comparing (44) with (42), one has:

$$\mathscr{P}_{k+1} = rI(a,r)\mathscr{P}_k,$$

and further

$$\mathscr{P}_k = (rI(a,r))^{k-2} a^r, \quad k = 2, 3, \dots$$

It can be proven (see Appendix 1), that $rI(a,r) < 1$ for $r > 0$, $0 < a < 1$. Thus, from (37) and (41) one has the following:

$$\bar{t} = \frac{2}{\lambda} + \frac{1}{\lambda}\sum_{m=2}^{\infty} a^r (rI(a,r))^{m-2} = \frac{2}{\lambda} + \frac{1}{\lambda}\frac{a^r}{1 - rI(a,r)}. \tag{46}$$

6 Discussion

We obtained here the ISI probability distribution function for the LIF neuron without usage of diffusion approximation. The diffusion approximation can be precise enough if a large number of input impulses is required for triggering, [3,4]. We considered here the case, which

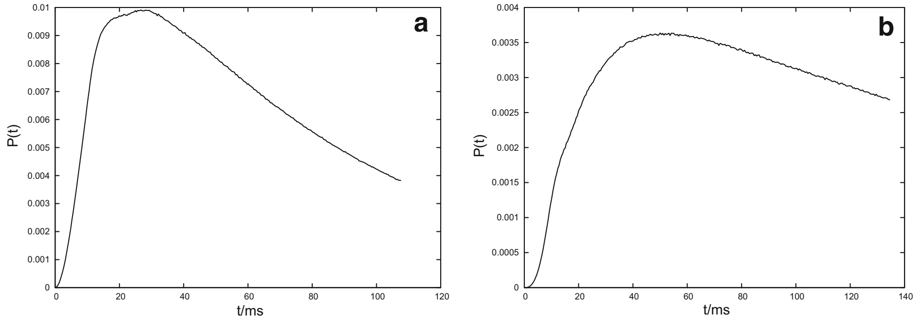

Fig. 4 Pdf of ISIs, $P(t)$, found numerically, by Monte Carlo simulation for the cases when at least three (**a**), and four (**b**) input impulses are required to trigger a spike. In **a** $h = 9.2$ mV, the total probability mass under the curve is 0.727. In **b** $h = 6.5$ mV, the total probability mass under the curve is 0.395. In **a** and **b**: $\lambda = 62.5$ s^{-1}, $\tau = 20$ ms, $V_0 = 20$ mV, the number of output spikes used in Monte Carlo calculation is 100,000,000

is least suitable for usage of diffusion approximation. Namely, the LIF can be triggered with two impulses obtained in a short sequence. This situation is observed for some real neurons [7,8].

The exact expression found for the pdf is different for different intervals of the whole range of ISI values, see (18), (31), and is presented by means of multiple integrals, see Eq. (22), (23). The multiple integrals are taken for the first three intervals, which allows to make some conclusions about qualitative course of the pdf.

First, it is not Poisson-like. The suitability of Poisson distribution for describing neuronal activity is discussed in neurophysiology, see, e.g. [12]. In our case, the evident deviation from exponential distribution near the short ISIs is because more then one (actually two at least) input impulses are required for triggering. This same deviation will be observed if more then two impulses are required, see Fig. 4.

Second, the obtained pdf for ISIs distribution has a local minimum at interval $]\Theta_3; \Theta_5]$ for some parameter values, see Fig. 2 and Appendix 2. This kind of minimum was not described earlier for calculations with pure diffusion processes, even if multimodality is often observed in experimental histograms.[2] Under diffusion approximation, an infinite number of input impulses is required for triggering, whereas in this paper already two input impulses delivered in a short sequence are able to trigger. This may be the reason of bimodality in Fig. 2. For mathematical models, which combine a diffusion process with random finite jumps, a multimodality was also observed, [3, Fig. 5.4], see also [13,14].

As regards the mean ISI, see Eqs. (45), (46), it is monotonously decreasing with increasing λ, as it might be expected.

If we have a look at Eqs. (2), (3) of paper [15] for binding neuron (BN), then it is possible to recognize their structural similarity with Eqs. (20), (23) here. This is because cond. (1) ensures that LIF neuron behaves similarly to the BN with threshold 2 in the context of calculation of contribution of individual events into the triggering probability.

It would be interesting to compare results obtained without diffusion approximation with those obtained with diffusion approximation. For this purpose it is necessary to obtain results without diffusion approximation in cases when not two, but many input impulses are required for triggering. This is not simple task and may be a subject of another paper. Material of this

---

[2] The main reason of multimodality for neurons embedded into a network is the presence of delayed feedback.

paper covers the area, where diffusion approximation does not hold, which makes a required comparison impossible.

Acknowledgements This paper was supported by the Program “Microscopic and phenomenological models of fundamental physical processes in a micro and macroworld” of the National Academy of Science of Ukraine, Project PK No. 0112U000056.

Appendix 1: Upper Bound

Theorem 3 *For integral defined in (45), the following estimate is valid:*

$$r > 0 \quad \wedge \quad 0 < a < 1 \qquad \Rightarrow \qquad rI(a, r) < 1.$$

Proof Expression $rI(a, r)$ increases with increasing a. Therefore, it is enough to prove the statement for $a = 1$:

$$r > 0 \qquad \Rightarrow \qquad rI(1, r) < 1,$$

or

$$r \int_0^{1/2} \frac{x^{r-1}}{1-x} dx < 1 \quad \text{if} \quad r > 0.$$

□

Here, the integral can be rewritten as follows:

$$r \int_0^{1/2} \frac{x^{r-1}}{1-x} dx = r \int_0^{1/2} \sum_{k \geq 0} x^{k+r-1} dx = r \sum_{k \geq 0} \frac{1}{k+r} \left(\frac{1}{2}\right)^{k+r}.$$

The last equality is approved by the fact that the integrand is a uniformly convergent series at the integration domain. The last expression can be transformed as follows:

$$\begin{aligned} rI\ &(1, r) \\ &= \left(\frac{1}{2}\right)^r \left(1 + r \sum_{k \geq 1} \frac{1}{k+r} \left(\frac{1}{2}\right)^k\right) < \left(\frac{1}{2}\right)^r \left(1 + r \sum_{k \geq 1} \frac{1}{k} \left(\frac{1}{2}\right)^k\right) \\ &= \left(\frac{1}{2}\right)^r (1 + r \log(2)) = \phi(r). \end{aligned}$$

The function $\phi(r)$ decreases strictly monotonically, and $\phi(0) = 1$. This completes the proof.

Appendix 2: Bimodality

In order the $P(t)$ to have a minimum at $[\Theta_3; \Theta_4[$ it is necessary that its first derivative has a zero at this interval. Taking into account (31) we have

$$\frac{d}{dt} P(t) = -\frac{e^{-\lambda t} \left(\lambda^4 T_2^2 + \left(4\lambda^3 - 2\lambda^4 t\right) T_2 + \lambda^4 t^2 - 2\lambda^3 t\right)}{2} = 0.$$

The smaller root, t_1 corresponds to a minimum here. Expression for it is as follows:

$$t_1 = \frac{\lambda\, T_2 + 1 - \sqrt{1 - 2\,\lambda\, T_2}}{\lambda}.$$

In order the t_1 to be real, we need $\lambda < 1/(2T_2)$, or, taking into account (1) and (13) one has

$$\lambda < -\frac{1}{2\tau \log(g-1)}, \quad \text{where } g = V_0/h, \quad 1 < g < 2. \tag{47}$$

In order the t_1 to fall into the $[\Theta_3; \Theta_4[$ we need $t_1 < T_2 + T_3$, or using additionally (14) one has

$$\lambda < 2\frac{\log(g)}{\tau(\log(g/(g-1)))^2}. \tag{48}$$

It can be estimated numerically that the inequality (47) follows from the inequality (48). Thus, the (48) gives the necessary and sufficient condition for the $P(t)$ to have a minimum at $[\Theta_3; \Theta_4[$. Actually (48) imposes limitation on the product $\lambda\tau$:

$$\lambda\tau < 2\frac{\log(g)}{(\log(g/(g-1)))^2}.$$

Here, the right hand side has a maximal value ~2.885 at $g = 2$. Thus, if the relation between V_0 and h is only specified by (1), then for h close to $V_0/2$ we have

$$\lambda\tau < 2.885.$$

References

1. Vidybida, O.K.: Output stream of leaky integrate and fire neuron. Rep. Natl. Acad. Sci. Ukr. **2014**(12), 18–23 (2014)
2. Stein, R.B.: Some models of neuronal variability. Biophys. J. **7**(1), 37–68 (1967)
3. Sacerdote, L., Giraudo, M.T.: Stochastic integrate and fire models: a review on mathematical methods and their applications. In: Bachar, M., Batzel, J.J., Ditlevsen, S. (eds.) Stochastic Biomathematical Models, Lecture Notes in Mathematics, pp. 99–148. Springer, Heidelberg (2013)
4. Ricciardi, L.M., Sacerdote, L.: The Ornstein–Uhlenbeck process as a model for neuronal activity. Biol. Cybern. **35**, 1–9 (1979)
5. Alili, L., Patie, P., Pedersen, J.L.: Representations of the first hitting time density of an Ornstein–Uhlenbeck process. Stoch. Models **21**, 967–980 (2005)
6. Andersen, P., Raastad, M., Storm, J.F.: Cold Spring Harbor Symposia on Quantitative Biology. Excitatory synaptic integration in hippocampal pyramids and dentate granule cells, pp. 81–86. Cold Spring Harbor Laboratory Press, Cold Spring Harbor (1990)
7. Miles, R.: Synaptic excitation of inhibitory cells by single CA3 hippocampal pyramidal cells of the guinea-pig in vitro. J. Physiol. **428**, 61–77 (1990)
8. Gulyas, A.I., Miles, R., Sík, A., Tóth, K., Tamamaki, N., Freund, T.F.: Hippocampal pyramidal cells excite inhibitory neurons through a single release site. Nature **336**(6456), 683–687 (1993)
9. Korolyuk, V.S., Kostyuk, P.G., Pjatigorskii, B., Tkachenko, E.P.: Mathematical model of spontaneous activity of some neurons in the cns. Biofizika **12**(5), 895–899 (1967)
10. Doob, J.L.: Stochastic Processes. Wiley, New York (1964)
11. Korolyuk, V.S.: Boundary Problems for Compound Poisson Processes. Naukova Dumka, Kiev (1975)
12. Averbeck, B.B.: Poisson or not poisson: differences in spike train statistics between parietal cortical areas. Neuron **62**(3), 310–311 (2009)
13. Sacerdote, L., Sirovich, R.: Multimodality of the interspike interval distribution in a simple jump-diffusion model. Sci. Math. Jpn. **58**(2), 307–321 (2003)
14. Sirovich, R., Sacerdote, L., Villa, A.E.P.: Cooperative behavior in a jump diffusion model for a simple network of spiking neurons. Math. Biosci. Eng. **11**(2), 385–401 (2014)
15. Vidybida, O.: Output stream of a binding neuron. Ukr. Math. J. **59**(12), 1819–1839 (2007)